

Article

Thermal Properties of Hemp Shives Used as Insulation Material in Construction Industry

Piotr Kosiński ^{1,*}, Przemysław Brzyski ², Maria Tunkiewicz ¹, Zbigniew Suchorab ^{3,*},
Damian Wiśniewski ¹ and Paweł Palczyński ¹

¹ Faculty of Geoengineering, University of Warmia and Mazury in Olsztyn, Jana Heweliusza 4, 10-724 Olsztyn, Poland; maria.tunkiewicz@uwm.edu.pl (M.T.); damian.wisniewski.3@student.uwm.edu.pl (D.W.); pawel.palczynski@student.uwm.edu.pl (P.P.)

² Faculty of Civil Engineering and Architecture, Lublin University of Technology, 40 Nadbystrzycka Str., 20-618 Lublin, Poland; p.brzyski@pollub.pl

³ Faculty of Environmental Engineering, Lublin University of Technology, 40B Nadbystrzycka Str., 20-618 Lublin, Poland

* Correspondence: piotr.kosinski@uwm.edu.pl (P.K.); z.suchorab@pollub.pl (Z.S.); Tel.: +48-81-538-47-56 (Z.S.)

Abstract: The article presents the results of studies concerning raw hemp shives obtained from the Polish crop of industrial hemp as a loose-fill thermal insulation material. The study focuses mainly on the measurements of the pore size distribution, thermal conductivity and air permeability of material. An increase in the value of the thermal conductivity coefficient (0.049–0.052 W/(m·K)) was demonstrated with an increase in the bulk density. The porosity of the individual pieces of shives is 78.7% and the predominant number of pores is in the diameter range of 0.9–3 μm. The paper also presents an example of the use of the tested material as thermal insulation of the wooden frame wall. The heat flow analysis was performed in various wall variants (insulation thickness: 100, 200 and 300 mm and pressure difference 0, 5, 10 and 15 Pa). A clear influence of the variables on the temperature distribution was observed.

Keywords: hemp shives; porosity; thermal conductivity; air permeability; building partitions



Citation: Kosiński, P.; Brzyski, P.; Tunkiewicz, M.; Suchorab, Z.; Wiśniewski, D.; Palczyński, P. Thermal Properties of Hemp Shives Used as Insulation Material in Construction Industry. *Energies* **2022**, *15*, 2461. <https://doi.org/10.3390/en15072461>

Academic Editors: Chi-Ming Lai and F. Pacheco Torgal

Received: 11 February 2022

Accepted: 25 March 2022

Published: 27 March 2022

Publisher's Note: MDPI stays neutral with regard to jurisdictional claims in published maps and institutional affiliations.



Copyright: © 2022 by the authors. Licensee MDPI, Basel, Switzerland. This article is an open access article distributed under the terms and conditions of the Creative Commons Attribution (CC BY) license (<https://creativecommons.org/licenses/by/4.0/>).

1. Introduction

Hemp shives are the wooden parts of the industrial hemp stem. These are fiber plants grown for the needs of various industries, including textile, food, pharmaceutical and construction. In Poland, these plants are cultivated for about 4 months. During this time, depending on the variety and sowing density, they can grow to a height of up to 4 m. From one hectare of cultivation, it is possible to obtain 6–9 tons of dry matter of hemp straw [1,2], of which about 75% is the wooden core of the stem yielding the shives [3,4]. Hemp needs large amounts of carbon dioxide to grow. One ton of dry matter in hemp yield can store 1000–2900 kg of CO₂ [1,5–7]. The straw as raw material has therefore a highly negative carbon footprint.

Construction is an energy-consuming branch of the economy. Energy consumption for construction processes and the use of buildings correspond to approximately 40% of total world energy usage [8]. Insulating materials used today, such as rock wool and polystyrene, have a high carbon footprint. It is reasonable to search for alternative insulation materials with minimal embodied energy. The use of semi-finished products obtained from straw (fiber and shives) in the production of building materials can significantly reduce the level of their embodied energy [4].

In the past century, they were usually treated as waste when obtaining the fiber from the stem. As waste, they were of poor quality. They contained a lot of dust, residues on fibers, whereas fractions were very irregular (e.g., presence of pieces several centimeters

long). Such shives are mainly used as bedding for animals, as they are highly hygroscopic and thus improve hygiene in animal husbandry rooms [1].

Hemp shives are currently used (since the 1980s [9]) in construction as a lightweight aggregate in composites based on lime, clay or magnesia binder. For this purpose, high quality of shives is required. They should be cleaned of dust (from plant and soil) as this increases the need for water and binder; moreover, they should be cleaned of fiber clumps (a small number of single, short fibers are recommended because they act as micro-reinforcement). Both finer and coarser fractions are used, but the shives mix should have an appropriate grading curve.

The shives in a dry form, without strict observance of the specified fraction and fiber content, can also be used as loose insulation in partitions in a wooden frame structure (insulation of walls, floors, ceilings and roofs). The effectiveness of the insulation will depend on the degree of shives density, which was confirmed in the tests on insulation made of flax shives [10]. The efficiency of loose insulation is both affected by thermal conductivity and prevention against wind washing or air filtration through the material. The air filtration can significantly reduce the thermal resistance of the thermal insulation layer [11]. Typically, this type of construction requires a wind barrier.

High porosity, in the range of 57–92% according to the literature [12–14], is one of the most characteristic features of shives. According to Collet et al. [15], the structure of hemp shives consists of a network of closed pores with a diameter predominantly from 5 to 50 μm . The pore walls of the shives are cellular. The cells in these walls are approximately 2.5 μm in diameter [15]. Various methods are used to determine the porosity of the shives. Jiang et al. [16] examined the porosity using the mercury porosimetry intrusion method, obtaining a result of $76.67 \pm 2.03\%$. It has also been found that testing with this method does not change the pore structure. The same shives were also tested for porosity by CT scanning (computed tomography), and a lower porosity of 50% was obtained. The reason was, among others, that this method only takes into account the pores larger than 2.54 μm . However, it gives more information about the shape of the pores and their interconnections in three dimensions. The pycnometric method was also employed to study the internal porosity, using toluene as a filling substance [17]. Depending on the method, the porosity of shives can be tested on selected single shives particles or on a compacted mixture of shives. In the latter case, the pore volume between the shives is also taken into account. However, the literature does not always provide the information on the preparation of a sample for porosity testing. The total porosity and pore size distribution depend on the variety of hemp from which the shives were obtained, as the stalks differ in terms of parameters. The structure may also be influenced by the method of retting and the treatment of the hemp stem to obtain shives. Therefore, it is important to measure the parameters of the shives that are going to be used in practice.

High porosity influences the low thermal conductivity, and thus makes the material applicable in building constructions. According to the literature [12,18–23], the thermal conductivity coefficient of shives is in the range of 0.048–0.058 $\text{W}/(\text{m}\cdot\text{K})$. This parameter is usually tested on a sample of shives thickened to a different degree using a plate apparatus [12,18,19]. When examining the material in this way, the thermal conductivity of the space between the shives is also taken into account. Tests are usually carried out on the shives dried to a constant weight. Balciunas et al. [12] proved that the shives seasoned in air-dry conditions, under the influence of air humidity, have a thermal conductivity 8.2–8.8% higher than the shives dried to constant weight. The direction of the capillary pores in relation to the heat flow stream also affects the thermal conductivity. The example of a hemp–lime composite showed that when the shives were arranged with fibers (and, also, capillaries) perpendicular to the heat flow, the composite was characterized by a lower thermal conductivity [24].

High porosity is responsible for the ability to absorb water. Arnaud et al. [25] proved that the shives are able to absorb significant amounts of water (2–3 times more in relation to the dry weight). After 10 min from immersion, their saturation reached 95%. Jiang et al. [16]

showed that the capillaries extend along the hemp stem (along the direction of the fibers), but the walls between the capillaries contain a perforation that allows moisture to pass between the capillaries. On the example of the study of the hemp–lime composite, it was found that the shives in which the capillaries will be located perpendicular to the water table show greater water uptake capacity. Placing the shives with capillaries parallel to the water table allowed for the reduction of water absorption by about 18%, despite the presence of the aforementioned perforation in the capillary walls [24].

The study investigated the physical properties of hemp shives from the crops of industrial hemp grown in Poland. They were tested for use as a loose thermal insulation material. The thermal conductivity, porosity and air permeability of shives with varying degrees of density were investigated. There are publications on the thermal behavior of hemp shives-based building materials [26–32], but it is difficult to find the analyses of shives properties such as correlation between density and thermal conductivity; in addition, there are no results on air permeability. Another novelty in the work will correspond to characterization of the pore size distribution of shives. The investigated thermal parameters were used to simulate a construction (various variants) filled with shives in the Delphin software (<http://bauklimatik-dresden.de> accessed on 11 February 2022).

2. Possible Applications of Shives in Construction Industry

In practice, hemp–lime composites are the main application of shives as lightweight aggregates. This composite may be used as the filling of the timber frame structure in the walls, floors and roof. It has a thermal conductivity coefficient in the range of 0.074–0.138 W/(m·K) [26–28] depending on the composition used, e.g., shives to lime ratio. The composite also has a high thermal capacity of the order of about 1000–1600 J/(kg·K) [29–32] which positively influences the preservation of heat in the walls, affecting the thermal comfort in the rooms.

Hemp aggregate is also used in the composites based on the magnesia binder. These composites, due to their greater strength than those based on lime, are used in the production of prefabricated elements. Their thermal conductivity also depends on the composition and can be, for example, 0.074–0.082 W/(m·K) [18,28].

Bricks consisting of clay and shives are also produced and researched scientifically. Depending on the density, their thermal conductivity can be in the range of about 0.09–0.18 W/(m·K) [33].

Shives with finer fractions, often in combination with hemp fibers, are used to make thermal-insulating mortars and plasters [34–36]. These additives also improve the resistance to shrinkage.

Hemp shives, such as flax shives [10], are used in their raw form as loose thermal insulation of partitions in a timber frame structure. In the past, shives dry mixed with lime or clay was used as insulation for ceilings.

3. Materials and Methods

3.1. Hemp Shives

The hemp shives of the Białobrzskie variety of the Polish producer Podlaskie Konopie (Białystok, Poland) were used for the research. They were obtained with the help of a small decorative line, but adapted to the production of high-quality hemp shives for construction purposes. They are characterized by a low content of dust and fibers. The shives used in the tests are shown in Figure 1a, while the shives length distribution is shown in Figure 1b. To determine the mass share of different ranges of shives lengths, 180 pieces of shives randomly selected from the mixture provided by the manufacturer were measured.



Figure 1. Hemp shives used in investigation (a) and their length (b).

The literature describes the studies in which shives of similar size were used [35]. The hemp shives of fractions 0–20 mm in length and a 4.4% proportion of length >20 mm in relation to the weight were tested. The largest share was constituted by the shives with a length of 5–10 mm.

3.2. Methods of Testing the Properties of Hemp Shives

3.2.1. Pore Size Distribution

The mercury porosimetry method was used to study the microstructure of hemp shives. Many authors indicate that the method of measuring porosity using mercury porosimetry is the right solution for the study of plant fibrous materials [16,37–39]. The porosity parameters were determined using the equation proposed by Washburn, which shows the relationship between the diameter of the pores and the pressure of mercury filling them (1):

$$R = - \frac{F\gamma \cos \theta}{p} \quad (1)$$

where R is radius of cylindrical pores (μm), F is shape factor (for cylindrical pore calculations equal to 2), γ is mercury surface tension (N/m), $\cos\theta$ is the limit value of the contact angle and p is the mercury pressure (MPa). The test is applicable to the materials with open porosity, incompressible with cylindrical pore characteristics [40]. The parameters determined during the study were: total porosity, total pore area, median pore diameter, bulk density and apparent density.

An Autopore Mercury Porosimeter (Atlanta, GA, USA) was used to investigate the pores in the range from 300 μm to 6 nm during two measuring cycles—in a low pressure station (measuring range 0.014 to 0.21 MPa) and in a high pressure station (from 0.21 to 227.53 MPa). The samples of the woody parts of hemp shives were prepared for the research. The initial selection of shives type was made in order to eliminate structures that could be damaged during the test. Before testing, the tested material was dried to a constant weight at a temperature of 60°C. The measurements were performed using a measuring vessel—designed for solid materials, with a capacity of 3 cm^3 . The weight of the samples was approximately 0.1872 g \pm 0.016 g. Three pieces of shives of different sizes were randomly selected for the porosity test. They are designated as HS1, HS2 and HS3.

3.2.2. Thermal Conductivity

The study was carried out in order to determine the value of thermal conductivity of loose hemp shives as a function of density. The thermal conductivity study was implemented on the basis of international standard EN 12667 [41]. The study was set up in the Laser Comp Fox 602 plate apparatus (TA Instruments, New Castle, DE, USA), the heat flow meter method.

The measuring space of the apparatus is defined by dimensions: 600 mm × 600 mm × 190 mm. The lower plate is stationary, while the upper plate is movable up and down. The highly sensitive digital sensor converters (heat meters) are mounted on the surfaces of both plates. The Fox 602 instrument operates on the basis of one-dimensional Fourier law (2):

$$q = -\lambda \frac{dT}{dx} \quad (2)$$

where q is the heat flux density flowing through the sample (W/m^2), λ is the thermal conductivity coefficient of the sample ($\text{W}/(\text{m}\cdot\text{K})$) and dT/dx is the temperature gradient on the isothermal flat surface of the sample (K/m).

The Fox 602 apparatus was calibrated before the measurements. The calibration sample (mineral wool) was certified by the Joint Research Centre, Institute for Reference Materials and Measurements in Geel, Belgium. According to the producer, the measuring uncertainty equals 1%.

Testing the samples involved placing them in a stabilizing frame. Every prepared sample (10 in total) was created by random selection of conditioned loose hemp shives. It was intentional to prepare the samples differing with density (from 109 to 124 kg/m^3). Every sample was tested 13 times. The loose material was placed evenly in the frame and subjected to initial manual compaction. The dimensions of the frame made of extruded polystyrene were as follows: 600 mm × 600 mm (external), and 520 mm × 520 mm (internal) as well as the height of 45 mm (Figure 2). Hemp shives are rigid enough to maintain the shape which was formed at the beginning of the measurement.



Figure 2. Heat flow meter—Fox 602 apparatus with hemp shives sample formed in the XPS frame.

In order to avoid condensation in the tested material, the shives samples were separated from the lower apparatus plate with a thin foil.

Then, the samples were compacted by the FOX 602. Due to the hardness of dry shives, it was only possible to achieve the density of material in the range 109–124 kg/m^3 . The measurements of the thermal conductivity coefficient were made at the average temperature of 10 °C, with 0 °C on the bottom plate and 20 °C on the top plate. The measurements were conducted automatically using the WinTherm32 software (<http://lasercomp.com> accessed on 11 February 2022). For each of the 10 prepared samples, 13 readouts of thermal conductivity coefficient were obtained.

3.2.3. Air Permeability

The study was carried out in order to determine the value of air permeability κ (m^2) of loose hemp shives in the function of density. The values of κ were determined on the basis of the Forchheimer equation, which is an extension of Darcy's law, describing the effect of a square resistance on the pressure drop across the porous medium. For flows characterized with Reynolds number greater than one, derogation from the Darcy law is experienced due

to the flow square resistance. This phenomenon is described by the Forchheimer equation presented by (3):

$$-\frac{dp}{dx} = \frac{\mu}{\kappa} \cdot v + \beta \cdot \rho \cdot v^2, \quad (3)$$

where dp is the pressure difference between pressure taps (Pa), dx is the distance between pressure taps (m), μ is the dynamic viscosity (Pa·s), κ is the air permeability coefficient (m²), β is the Forchheimer coefficient (1/m), ρ is the fluid density (kg/m³) and v is the velocity of fluid flow (m/s).

The measuring system (Figure 3) was constructed based on previous investigations of many researchers, which is described in detail in the work [42].



Figure 3. The apparatus for air permeability measurements filled with hemp shives.

Pressure difference was measured by a Testo 435-4 electronic differential pressure gauge (produced by Testo SE & Co. KGaA, Titisee-Neustadt, Germany), with measuring range 0–25.0 hPa and resolution 0.01 hPa. Air velocity was recorded by a TA7 thermoanemometer (produced by Airflow Developments Limited, High Wycombe, UK) with measuring range 0–2.0 m/s and resolution 0.01 m/s. Air was compressed in the screw compressor, equipped with the filter and dryer, and delivered to the apparatus by a pressure reducer.

Testing the samples involved placing them in a central part of the system. Every prepared sample was created by random selection of conditioned loose hemp shives. The authors prepared the samples differing with density, from 90 to 120 kg/m³ with 5 kg/m³ resolution. During the measurements, the pressure difference between two taps, located in central part of the apparatus, was registered. Simultaneously, air velocity on the exhaust was registered. In order to avoid discrepancy of the density and viscosity of the air during investigation, a constant temperature +10 °C of compressed air was maintained. Every single calculated value of permeability was determined from the approximation of (3) on the basis of at least 800 pairs of air velocities and air pressures.

Due to the technical declaration of producers, the standard measurement uncertainty of the pressure difference is ± 2 Pa in the measuring range, while the uncertainty of air velocity is ± 0.04 m/s. Pressure uncertainty can be practically neglected in the achieved range (up to 6000 Pa) of the pressure difference, but the uncertainty of air velocity is very important. The authors estimated this influence: underestimation of air velocity can result in up to 29% overestimation of air permeability, while overestimation of air velocity can lead up to 55% of underestimation of air permeability.

4. Results and Discussion

4.1. Pore Size Distribution

After conducting the tests of open porosity on three samples of hemp material, the curves of the cumulative intrusion volume were obtained, presented in Figure 4. The characteristics of the pore distribution curves in all tested samples were similar. The highest total porosity was found in the HS1 sample, while the smallest in the HS2 sample. From

the cumulative intrusion vs. pore size figure, it can be clearly seen that the material pore dimensions range between 50 and 0.08 μm .

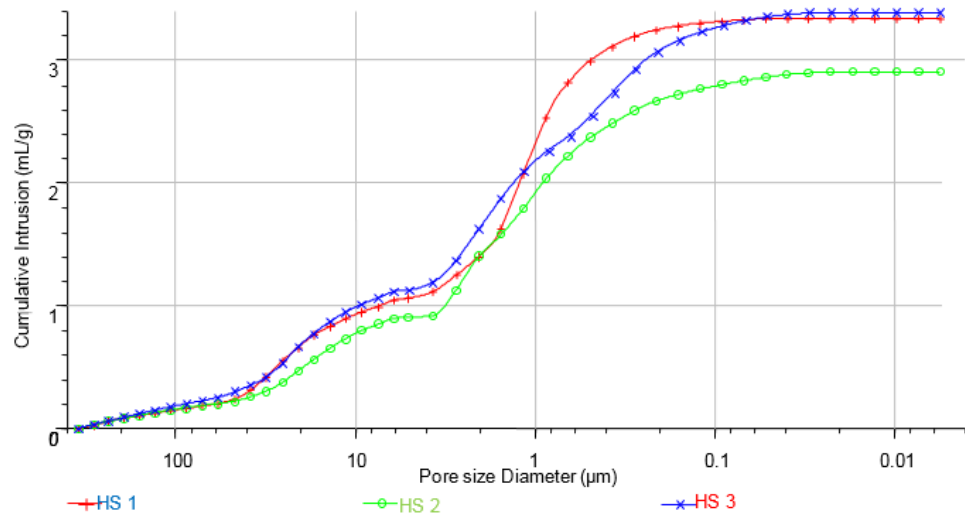


Figure 4. Cumulative intrusion vs. pore size diameter (μm).

On the basis of the analysis of the obtained results (Figure 5.) the domination of pores in the range of 3–0.9 μm is visible, their share is about 40% of the total porosity. An additional peak is seen in the range of 50–10 μm . The pores in the range of 0.9–0.1 μm account for about 30% of the total porosity. The smallest pores in the range from 0.08 μm constitute a small share.

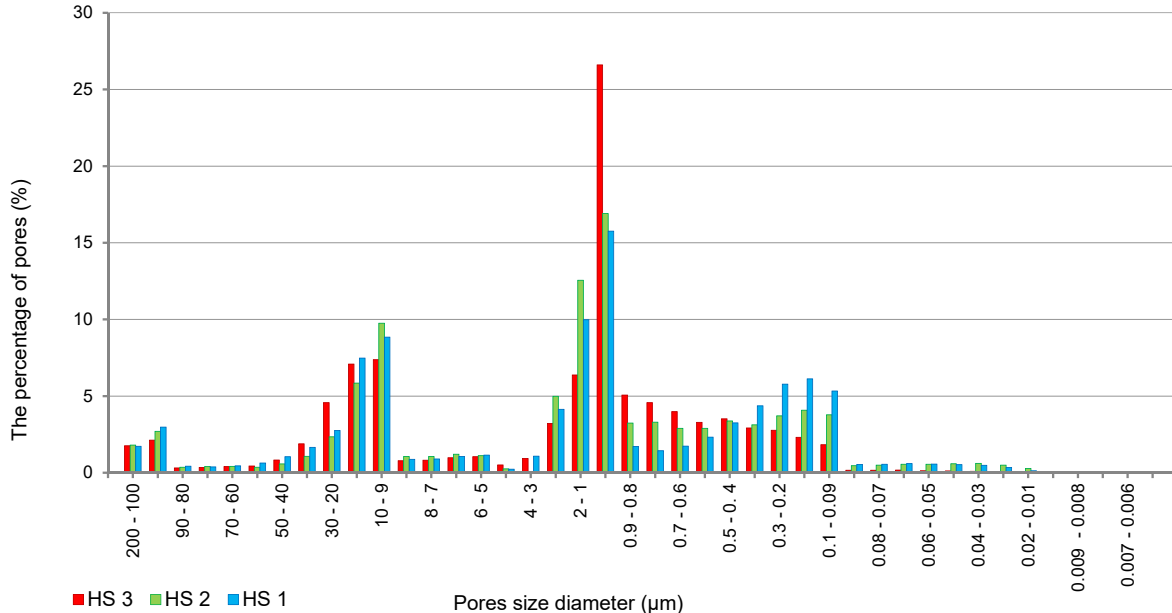


Figure 5. The percentage of the pores vs. pore size diameter (μm).

The additional parameters determined by the measuring device are summarized in Table 1. The total porosity is $78.70\% \pm 1.65\%$. The bulk density is about 0.25 g/cm^3 . The median pore diameter is approx. $1754.2 \text{ nm} \pm 280 \text{ nm}$. Bourdot et al. [13] showed higher values of porosity of hemp shives and the influence of shives length on porosity. The 0–5 mm shives were characterized by the porosity of 89.3%, while the shives of the 5–20 mm length were characterized by the porosity equal to 91.3%. Rahim et al. [14] also showed a higher porosity of shives, equal to 90.1%. However, this study does not provide a methodology for testing porosity. It is possible that these results relate to the porosity of the

compacted shives sample and that the volume of the pores between the shives is also taken into account. In the authors' own research, the results concern only shives (three randomly selected shives: HS1, HS2 and HS3).

Table 1. Structure characteristics determined by mercury porosimetry.

Hemp Shives Type/Property	HS1	HS2	HS3	Unit
Total Intrusion Volume	3.34	2.9132	3.3908	mL/g
Total Pore Area	13.586	21.309	24.948	m ² /g
Median Pore Diameter (Volume)	1476.4	1897.1	1889.1	nm
Bulk Density	0.2406	0.2625	0.2338	g/mL
Porosity	80.346	76.4842	79.269	%

4.2. Thermal Conductivity

Figure 6 presents the results of measurements of the mean thermal conductivity coefficient of 10 samples with different bulk densities. The range of achieved density was: 109–124 kg/m³. The obtained mean thermal conductivity coefficients of tested samples were in the range 0.049–0.052 W/(m·K) with a little tendency to rise with density. This tendency may be due to reducing the pore size between separate shives. Along with reducing the pore size between the shives, the effect of heat transport by convection is reduced [43].

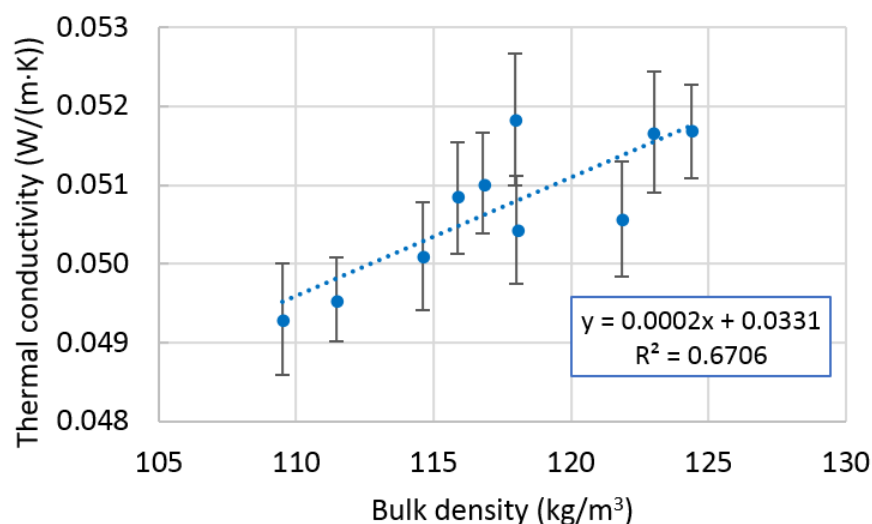


Figure 6. Thermal conductivity of hemp shives for different achieved bulk densities of samples (error bars mean standard deviation).

Delhomme et al. [44] tested the thermal conductivity of the shives with a bulk density of 106 kg/m³ and 138 kg/m³, obtaining the results of 0.079 W/(m·K) and 0.1 W/(m·K), respectively. However, these were the shives with a smaller fraction (over 80% of the shives mixture mass passed through a sieve with a mesh of 4.75 mm). Balcianus et al. [12], on the other hand, tested the mixtures of shives with various ranges of 2.5–5 mm, 5–10 mm and 10–20 mm. The thermal conductivity of the shives in a dry state was 0.053 W/(m·K), 0.055 W/(m·K) and 0.059 W/(m·K), respectively. Other papers also confirm that the results of thermal conductivity are quite varied. Different types of hemp, different structure, pore distribution and fraction make it possible to obtain significantly different results of thermal conductivity by examining two different mixtures of shives with the same bulk density (Table 2). The obtained own results of the thermal conductivity coefficient are similar to those presented in Table 2; however, they provide a broader view of the variability of this parameter depending on the bulk density of the one type of shives.

Table 2. Thermal conductivity of hemp shives, a literature review.

Bulk Density (kg/m ³)	Thermal Conductivity Coefficient (W/(m·K))	Literature
72.3	0.052	[19]
111.8	0.058	[20]
108.4	0.058	[18]
110.0	0.048	[21]
155.0	0.058	[21]
134.8	0.055	[22]
148.3	0.056	[23]

Unfortunately, the cited publications did not investigate the pore size distribution. Brzyski et al. [10] studied the dependence of the thermal conductivity of flax shives on the degree of compaction. The shives with a density of 131–159 kg/m³ were characterized by a thermal conductivity coefficient in the range of 0.047–0.053 W/(m·K). No clear relationship was found.

The discrepancy in the results presented in this section is related to different varieties and fractions of shives, but also to their anisotropic properties. It is a material with directed fibers (the direction of the fibers is in the direction of the growth of the hemp stalk (Figure 7)). A sample of shives subjected to the thermal conductivity test contains random shanks. In an article by Brzyski et al. [24] it was proven that the composite based on limestone binder and hemp shives, compacted parallel to the heat flux, was characterized by a thermal conductivity coefficient lower by 12–16% (depending on the fraction of shives) compared to the composite compacted perpendicular to the direction of heat flow.

**Figure 7.** Fiber orientation in hemp shives.

4.3. Air Permeability

Registered pressure drops and air velocity corresponding to them were used in the approximation of the Forchheimer equation (Equation (3)) to determine the air permeability coefficient κ of hemp shives. Different densities in the range of 90 ÷ 120 kg/m³ were investigated. The samples with higher density showed better resistance to air filtration. It is well seen by increasing the pressure difference with increasing density of the material. The results of the air permeability for investigated densities of hemp fibers are shown in Table 3.

Table 3. Results of the air permeability for investigated densities of hemp shives.

Bulk Density of Hemp Shives (kg/m ³)	Measured Maximum Pressure Difference On the Length of Specimen (Pa)	Measured Maximum Air Velocity in the Outlet of Apparatus (m/s)	Calculated Air Permeability Coefficient κ (m ²)
90	726	0.4	4.259744×10^{-8}
95	802	0.37	2.184845×10^{-8}
100	810	0.31	1.507439×10^{-8}
105	926	0.3	9.252043×10^{-9}
110	976	0.26	6.621214×10^{-9}
115	979	0.23	2.223948×10^{-9}
120	981	0.22	1.832226×10^{-9}

Air permeability coefficient for the hemp shives sample with the lowest density is $4.259744 \times 10^{-8} \text{ m}^2$ and for the sample with the highest density is $1.832226 \times 10^{-9} \text{ m}^2$. The air permeability coefficient values decrease with increasing density of material. The same relationship, except for selected single measurements, was observed in other studies [45–47]. Brzyski et al. investigated the air permeability of other insulation materials in the form of cellulose in the 30–70 kg/m³ density range. The air permeability coefficient was from $2.209767 \times 10^{-7} \text{ m}^2$ to $2.896716 \times 10^{-10} \text{ m}^2$, respectively [45]. In another work [46], insulation from loose, unprocessed hemp fibers in the density range of 25–70 kg/m³ was investigated. The obtained results are closer to those of hemp shives, between $9.775609 \times 10^{-8} \text{ m}^2$ and $1.053169 \times 10^{-8} \text{ m}^2$.

4.4. An Impact of Convection on Heat Transfer through Hemp Shives Insulation

Convection plays a significant role in heat transfer in the porous structures. Mostly, this effect is considered in thermal insulations, as they have the highest thermal resistance within the whole building element. The convection effect is smaller if the pores between the fibers are closed due to material compacting. While it is possible to easily compact straw materials [48] it is not in the case of hard shives. In the presented laboratory measurements, the authors did not manage to compact hemp shives more into the 124 kg/m³ density. This is why the convection analysis is important in this work.

The effect of convection on heat transfer in porous structures is described with the Rayleigh (Ra) number. The Rayleigh number relating to fibrous materials can be described as (4):

$$Ra = \frac{\beta \cdot g \cdot \delta \cdot \kappa \cdot (\rho c_p)}{\nu \cdot \lambda} \cdot \Delta T \quad (4)$$

where β is the thermal expansion coefficient (1/K), g is the gravity acceleration (m/s²), δ is the insulation thickness (m), κ is the air permeability coefficient (m²), ρ is the dry air density (kg/m³), c_p is the specific heat of dry air (J/(kg·K)), ν is the kinematic viscosity (m²/s), λ is the thermal conductivity coefficient of dry air (W/(m·K)) and ΔT is the temperature difference on both sides of insulation (K).

It is assumed that the heat transfer through the structures is based mainly on conduction if the Ra number is below a certain critical value. If the Rayleigh number is above the critical value, then the heat flow is mainly by convection.

According to ISO 10456 [49], it is recommended to include convection in heat transfer calculations for Ra number higher than 2.5 in the horizontal direction, in the vertical direction downwards $Ra > 30$, and in the vertical direction upwards $Ra > 15$.

On the basis of Formula (4), it could be concluded that convection takes part in heat exchange only in porous insulations with high air permeability, in thick layers and additionally with a high temperature difference. In fact, the contribution of forced convection in the heat transfer process in fibrous thermal insulation depends solely on the air permeability of the material and the exposure of the material to the air stream.

On the other hand, due to the increasing thermal requirements for building elements, thus, decreasing permissible heat transfer coefficients, the thermal insulation will be sig-

nificantly thicker. It will additionally increase the share of possible convection in the heat transfer. For this reason, it is worth analyzing the Ra number in the designed buildings insulated with air-permeable materials.

Figure 8 presents the calculated values of Ra number for different densities of thermal insulation made of loose hemp shives for 3 different thickness of the insulation: 100, 200 and 300 mm. The analysis of the values shows that as the density increases, the Rayleigh number and thus the share of convection in heat transfer in the insulation decreases. The maximal calculated Ra numbers for 90 kg/m³ density of hemp shives are: 8.94 for 100 mm, 17.88 for 200 mm and 26.82 for 300 mm, but minimal calculated for 120 kg/m³ are in the range 0.385–1.154. It shows how large is the impact of density on the possible air filtration in loose material. It should be noted that even if the Ra number is smaller than the critical values pointed in the ISO 10456 [49] standard, air filtration may occur in the insulation with any pressure difference. The detailed analysis is presented in the next section.

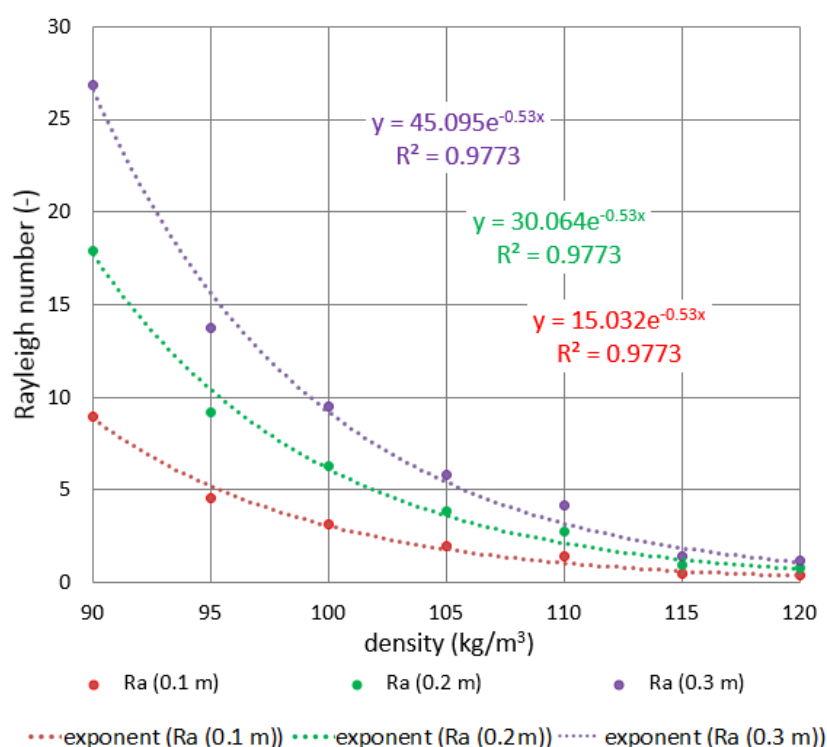


Figure 8. Dependence of the Rayleigh number on the density and thickness of thermal insulation made of hemp shives.

5. Thermal Simulation

5.1. Preprocessing

The thermal simulations were performed to present the hemp shives properties as thermal insulation in wooden frame construction. The simulations were performed using Control Volume Method in the Delphin 6.1 software, under steady state conditions in two cases: no air filtration and air filtration through the entire element.

Physical data for the simulation were adopted on the basis of laboratory measurements, presented in the article. The physical properties of materials, laboratory investigated are presented in Table 4.

Table 4. Physical properties of materials used in the simulation.

Material	d (m)	λ (W/(m·K))	κ (m ²)
Gypsum board	0.012	0.2000	-
OSB board	0.02	0.1300	-
Hemp shives 110 kg/m ³	0.1; 0.2; 0.3	0.0513	6.621×10^{-9}
Hemp shives 120 kg/m ³	0.1; 0.2; 0.3	0.0498	1.832×10^{-9}

The simulation model (Figure 9) corresponds to a wood frame wall filled with loose hemp fibers. Two examples differing in shives density were investigated: 110 and 120 kg/m³.

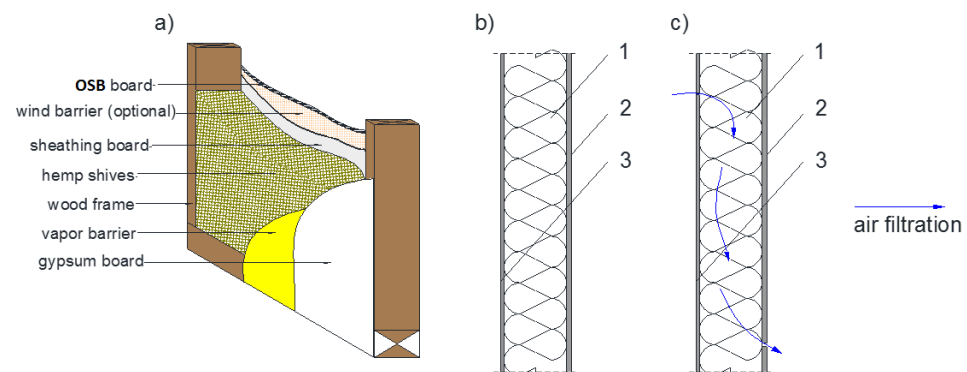


Figure 9. Cross-section of the simulation model, wall filled with hemp shives: (a) overall cross section, (b) no filtration case and (c) air infiltration case, 1—loose hemp shives (110 or 120 kg/m³), 2—gypsum board and 3—OSB.

For each density, three cases were modelled: wall with insulation thickness of 0.1, 0.2 and 0.3 m. For each thickness 4 conditions were applied: steady state conditions without air filtration and three cases of air filtration through the entire wall with pressure differences: 5, 10 and 15 Pa. The model consists of three layers: OSB from outside (0.02 m), loose insulation made of hemp shives (0.1, 0.2 and 0.3 m) and gypsum board from inside (0.012 m). The models height is 1.0 m. Automatic discretization of models with stretch factor 1.3 divided them into 3232 elements for the model with a thermal insulation thickness of 0.1 m as well as 0.2 m, and 3542 for the model with a thickness of 0.3 m.

Only temperatures and pressure difference were set in the model. The external temperature corresponds to the computational temperature of Warsaw: $t_e = -20.00$ °C, internal as for living room $t_i = 20.00$ °C, while pressure difference $\Delta p = 0.00, 5.00, 10.00$ and 15.00 Pa correspond to possible conditions during wintertime. The pressure difference is subjected to 2 mm leakages situated 100 mm from the bottom and the top of the model.

5.2. Model Description

The energy balance is given with the Equation (4) is described in detail in [46].

$$\frac{\partial}{\partial t}(\rho U) = \nabla \cdot \left(\lambda \nabla T + \kappa \frac{c_p \Delta T}{\nu} (\nabla p + \rho_g g) \right) + \rho_r \quad (5)$$

where ρU is the internal energy density (J/m³), λ is the heat conduction coefficient (W/(m·K)), ∇T is the temperature gradient (K/m), κ is the intrinsic permeability of a porous medium (m²), c_p is the specific heat of dry air (J/(kg·K)), ΔT is the temperature difference (K), ν is the kinematic viscosity of air (m²/s), ∇p is the pressure gradient (Pa/m), ρ_g is the dry air density (kg/m³), g is the gravity acceleration (m/s²) and ρ_r is the internal heat source density (W/m³).

5.3. Simulation Results and Discussion

Figures 10–12 present the heat flux profiles through the wall model depending on the thickness of the insulation (100 mm, 200 mm and 300 mm), density of hemp shives insulation (110 kg/m³ and 120 kg/m³) and air pressure (0 Pa, 5 Pa, 10 Pa and 15 Pa). The averaged heat flux was calculated for the internal surfaces of the model. The graphs show the period of 42 h, because this is the maximum time of stabilization of the heat flux flow (in the case of 300 mm thickness of the insulation—see Figure 12). In most cases, the stabilization was much faster, but in all cases the same period was used for comparative purposes.

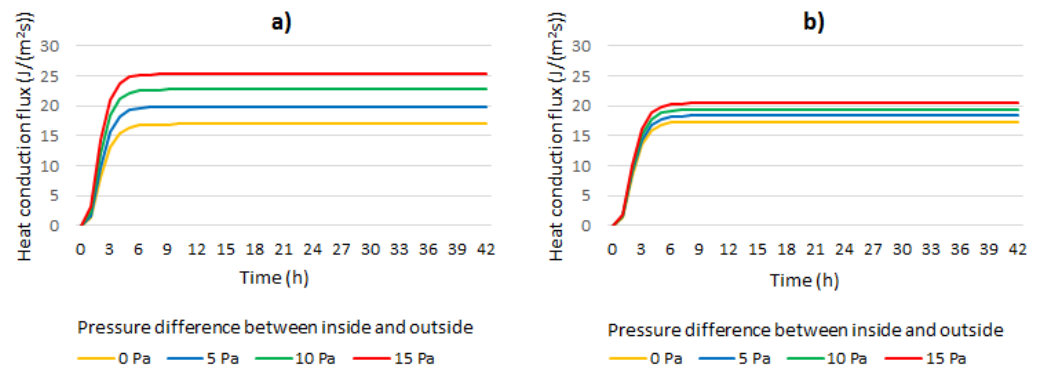


Figure 10. Heat conduction flux through the wall with 100 mm thickness of hemp fiber insulation with density of: 110 kg/m³ (a) and 120 kg/m³ (b).

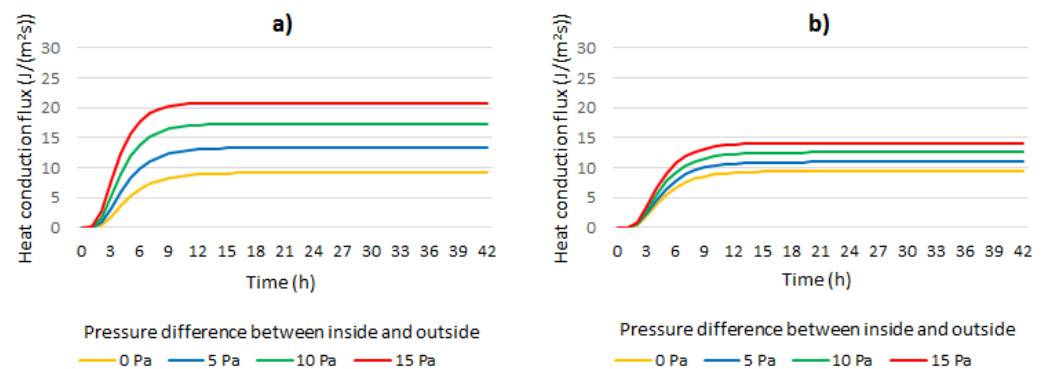


Figure 11. Heat conduction flux through the wall with 200 mm thickness of hemp fiber insulation with density of: 110 kg/m³ (a) and 120 kg/m³ (b).

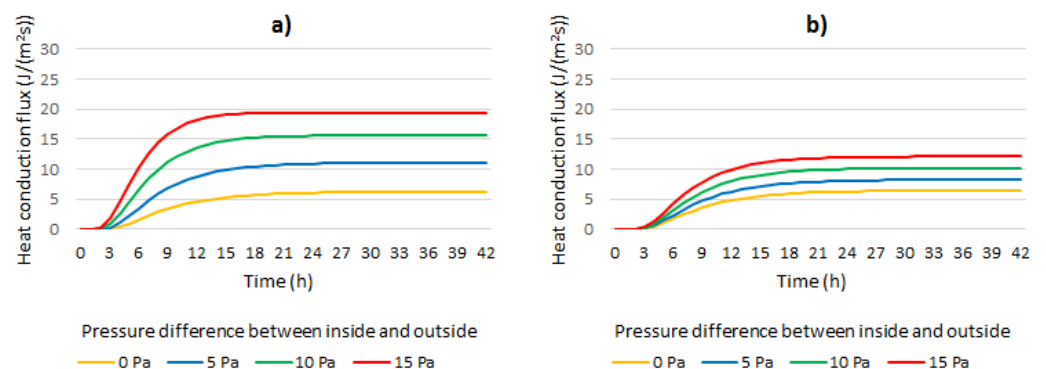


Figure 12. Heat conduction flux through the wall with 300 mm thickness of hemp fiber insulation with density of: 110 kg/m³ (a) and 120 kg/m³ (b).

In the presented figures (Figures 10–12) it can be clearly seen that air filtration causes the rise of heat fluxes for both analyzed densities of hemp shives, in the case of all thicknesses. Comparing the two tested insulation densities, it is visible that for a lower density,

the increase in heat flux occurs more rapidly after air filtration begins. The higher the pressure difference, the faster the changes occur. The heat fluxes depending on the pressure difference also reach higher values in this case. This is due to greater air permeability. For both densities, there is a tendency that as the thickness of the insulating material increases, the increase in the heat flux value takes longer to reach the maximum. This is characteristic of loose materials subjected to air filtration. Similar observations in the case of laboratory tests on blowing loose mineral wool were made by Kosiński et al. [50]. It is worth noticing that in the no-filtration cases, the difference between the results is no higher than 3% in the corresponding insulation thicknesses. The difference between the results is up to 62% in the air filtration cases.

The dependences of the heat flux on the pressure difference was analyzed. They were made for two thicknesses (100 and 300 mm) of insulation and two material densities of 110 and 120 kg/m³ (Figures 13 and 14). The abscissa axis shows the values obtained for the reference variant, without the pressure difference on both sides of the wall, and on the ordinate axis the values of the heat flux at the following pressure differences on both sides of the wall: 5, 10 and 15 Pa. The data are presented for a time interval of 70 h with an interval of one hour.

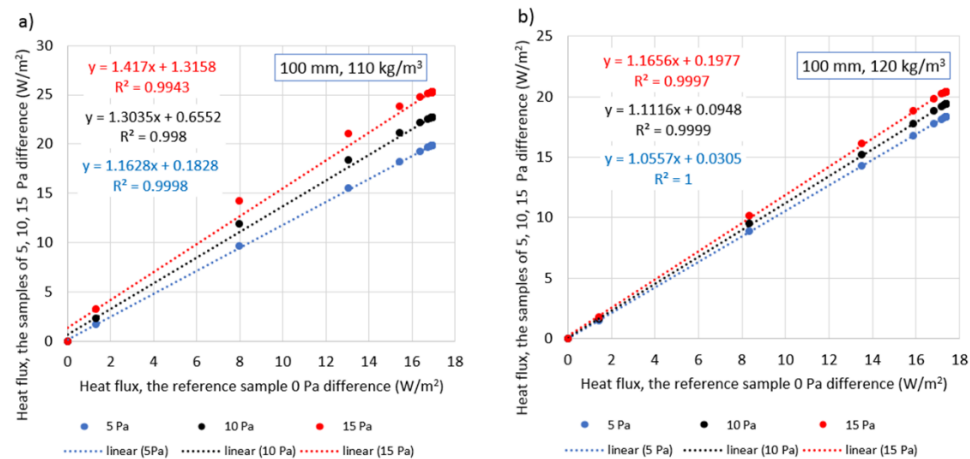


Figure 13. Comparison of the dependence of the heat flux in a wall with 100 mm insulation thickness on the pressure difference in the form of a comparison of the reference variant (0 Pa) with variants with a pressure difference of 5, 10 and 15 Pa, for a density of 110 kg/m³ (a) and 120 kg/m³ (b).

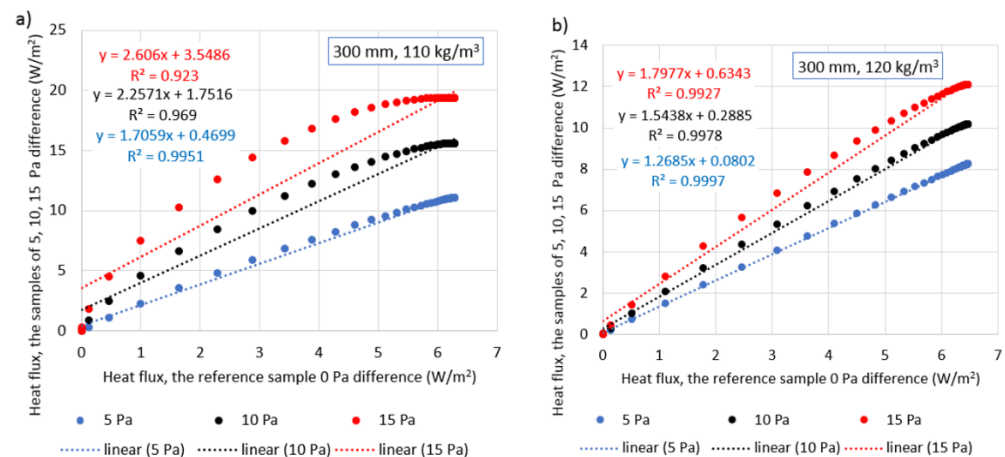


Figure 14. Comparison of the dependence of the heat flux in a wall with 300 mm insulation thickness on the pressure difference in the form of a comparison of the reference variant (0 Pa) with the variants characterized by a pressure difference of 5, 10 and 15 Pa, for a density of 110 kg/m³ (a) and 120 kg/m³ (b).

It was found that the increase of the pressure gradient on both sides of the simulated wall has a great influence on the heat exchange flux. In a model with a small thickness (100 mm) of insulation, this difference is smaller than in the case of a thicker insulation (300 mm). In the case of the insulation with a density of 120 kg/m^3 , the increase in flux over time was linearly proportional to the reference flux (at 0 Pa), and the maximum values obtained after the longest exposure time did not exceed 3 W/m^2 (18%) compared to the initial state. In the case of the insulation with a density of 110 kg/m^3 , the differences were more significant and for the 15 Pa pressure gradient reached 49%, it should be noted that after a period of about 8 h the differences are constant in relation to each other.

In the case of a thicker wall (Figure 14), the influence of the pressure difference is more pronounced. For higher density insulation, a linear dependence of the heat flux was found, different to the reference situation (0 Pa pressure gradient). It was found that for the 15 Pa pressure gradient, the difference between the heat fluxes were 88%, and for the density 110 kg/m^3 it was 309%.

Figure 15 presents the temperature distribution in the 110 kg/m^3 model for three different insulation thicknesses: 100, 200 and 300 mm in the case of no air filtration and the filtration caused by different air pressure: 5 Pa, 10 Pa and 15 Pa.

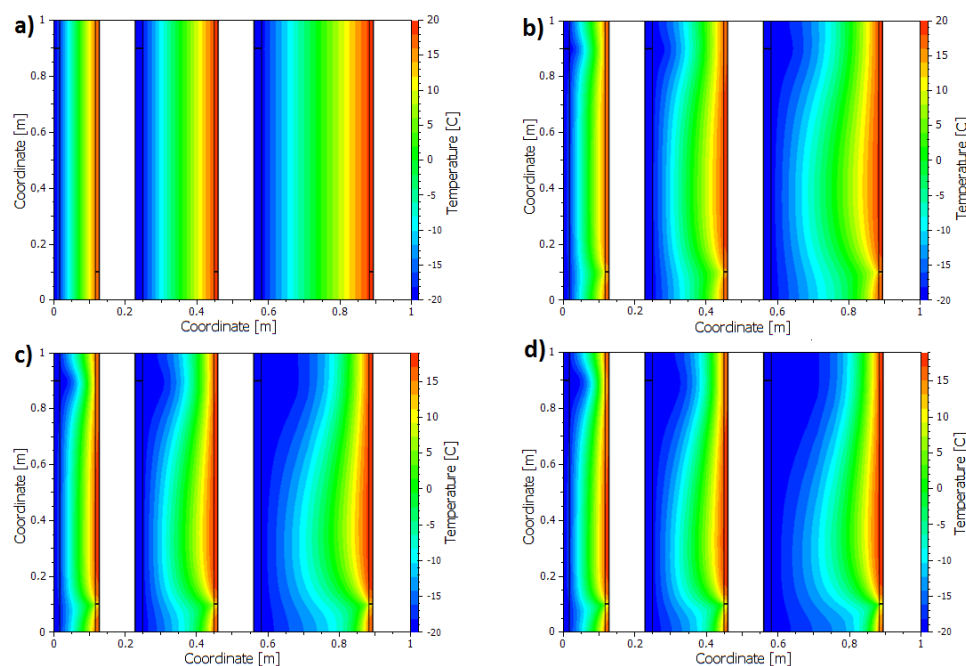


Figure 15. The temperature distribution in the 110 kg/m^3 models: no filtration (a), 5 Pa pressure difference (b), 10 Pa pressure difference (c) and 15 Pa pressure difference (d).

The temperature distribution presented in Figure 15 indicates the range of changes in heat distribution in the frame walls insulated with loose hemp shives subjected to air filtration. It is clearly visible that with the rising air pressure, the larger area of the model is affected by the cold outside air. Interestingly, the changes in the internal temperature distribution for the thinnest insulation model appear to be the smallest.

The analysis of the temperature changes on the internal surface in the contact point between the leakages and the gypsum board show a clear influence of the wind pressure on the temperature drop on the inner surface of the wall. Larger temperature drops were observed in the wall with the shives of lower density. This is understandable, because the looser structure of the insulation results in larger spaces between the shives, which allows the wind to flow more easily. The temperature drop in all cases occurs in direct proportion to the increase in wind pressure. At the strongest wind action, the temperature dropped, depending on the thickness of the glass, to $9.6\text{--}11.2 \text{ }^\circ\text{C}$ for a wall comprising the shives with density of 110 kg/m^3 and to $15.3\text{--}15.6 \text{ }^\circ\text{C}$ for a wall insulated with the shives characterized

by density of 120 kg/m^3 . The temperature without filtration was $17.9\text{--}19.2 \text{ }^\circ\text{C}$ for a wall comprising the shives with density of 110 kg/m^3 and $17.1\text{--}18.3 \text{ }^\circ\text{C}$ for a wall with the shives characterized by density of 120 kg/m^3 . Interestingly, in the case of a wall insulated with the shives of lower density, the temperature decreased as the wall insulation thickness increased. The temperature stabilization time is comparable (approx. 10 h), regardless of the wind pressure.

In another study [10], the temperature on the inner surface of a flat roof insulated with flax shives (lambda value equals $0.049 \text{ W/(m}\cdot\text{K)}$ and density equals 145 kg/m^3) with a layer thickness of 15 cm, 20 cm, 25 cm and 30 cm were investigated. The temperature ranged from $18.6 \text{ }^\circ\text{C}$ to $19.3 \text{ }^\circ\text{C}$ with $-20 \text{ }^\circ\text{C}$ outside and $20 \text{ }^\circ\text{C}$ inside. However, the influence of the wind was not taken into account in these analyses.

6. Conclusions

The research on the selected physical properties of hemp shives as the natural thermal insulation material enabled formulating the following conclusions:

- Thermal conductivity $0.049\text{--}0.052 \text{ W/(m}\cdot\text{K)}$, measured in the density range of $109\text{--}124 \text{ kg/m}^3$, shows a little tendency to rise with density. The density of 109 kg/m^3 was the minimum value that could be achieved with this test.
- Air permeability in the range of $4.259744 \times 10^{-8}\text{--}1.832226 \times 10^{-9} \text{ m}^2$, measured in the density range of $90\text{--}120 \text{ kg/m}^3$, shows a decreasing tendency with increasing density. The density of 90 kg/m^3 was the minimum value that could be achieved with this test.
- The porosity tests showed that the individual elements of the hemp shives have a porosity of more than 78%. The largest share, i.e., about 40%, corresponds to the pores with a diameter in the range of $0.9\text{--}3 \text{ }\mu\text{m}$.
- The results of the Rayleigh number calculation show that along with the rising density of shives, the share of convection will be limited. However, the results of the simulations indicate that in order to minimize the heat losses caused by convection, the thermal insulation made of shives should be covered with air-tight membranes.

The tested physical parameters, depending on the density of the shives mixture, made it possible to simulate the heat flux through a partition insulated with shives of different density. On the basis of the simulation results, the following conclusions were drawn:

- In the case of insulation with lower density, the increase in heat flux occurs more rapidly after air filtration begins. An increase in the pressure difference enhances the rate of changes. The maximum value of heat flux is reached after a longer time, the thicker the insulation is.
- Larger temperature drops on the inner surface of the wall, due to the air pressure were observed in the wall with shives of lower density.

The results of these studies indicate that hemp shives can be used well as a loose fill thermal insulation material in frame constructions. Currently, the authors continue the research on determining the moisture properties of hemp shives. The results, combined with simulation calculations will give broader view of the performance of loose hemp shives in constructions.

Author Contributions: Conceptualization, P.K. and P.B.; methodology, P.K., P.B. and M.T.; software, P.K. and M.T.; validation, P.K., P.B. and M.T.; formal analysis, P.K., P.B. and M.T.; investigation, P.K., M.T., D.W. and P.P.; resources, P.K. and P.B.; data curation, P.K., P.B. and M.T.; writing—original draft preparation, P.K., P.B. and M.T.; writing—review and editing, P.K., P.B. and Z.S.; visualization, P.K., P.B. and M.T.; supervision, P.K., P.B. and Z.S.; project administration, P.K. and P.B.; funding acquisition, Z.S. All authors have read and agreed to the published version of the manuscript.

Funding: This research was funded by Polish Ministry of Education within the grant number FD-20/IS-6/035.

Institutional Review Board Statement: Not applicable.

Informed Consent Statement: Not applicable.

Data Availability Statement: Data is contained within the article.

Conflicts of Interest: The authors declare no conflict of interest.

References

1. Van der Werf, H.M.G. Life cycle analysis of field production of fibre hemp, the effect of production practices on environmental impacts. *Euphytica* **2004**, *140*, 13–23. [CrossRef]
2. DEFRA. *UK Flax and Hemp Production: The Impact of Changes in Support Measures on the Competitiveness and Future Potential of UK Fibre Production and Industrial Use*; Department for Environment Food and Rural Affairs: London, UK, 2005.
3. Ip, K.; Miller, A. Life cycle greenhouse gas emissions of hemp-lime wall constructions in the UK. *Resour. Conserv. Recycl.* **2012**, *69*, 1–9. [CrossRef]
4. Zampori, L.; Dotelli, G.; Vernelli, V. Life cycle assessment of hemp cultivation and use of hemp-based thermal insulator materials in buildings. *Environ. Sci. Technol.* **2013**, *47*, 7413–7420. [CrossRef]
5. Boutin, M.-P.; Flamin, C.; Quinton, S.; Gosse, G. *Analyse du cycle de vie de mur en béton chanvre banché sur ossature en bois (Life Cycle Analysis of A Cast Hemp-Lime Timber Framed Wall)*; INRA: Lille, France, 2005.
6. Lawrence, M.; Fodde, E.; Paine, K.; Walker, P. Hygrothermal performance of an experimental hemp-lime building. *Key Eng. Mater.* **2012**, *517*, 413–421. [CrossRef]
7. Pervaiz, M.; Sain, M.M. Carbon storage potential in natural fiber composites. *Resour. Conserv. Recycl.* **2003**, *39*, 325–340. [CrossRef]
8. International Energy Agency (IEA). SHC Task 40/ECBCS Annex 52 towards Net-Zero Energy Solar Buildings 2013 Highlights. 2013. Available online: <http://task40.iea-shc.org/data/sites/1/publications/Task40-Highlights-2013.pdf> (accessed on 17 May 2018).
9. Allin, S. *Building with Hemp*; Seed Press: Kenmare, Ireland, 2012.
10. Brzyski, P.; Kosiński, P.; Zgliczyńska, A.; Iwanicki, P.; Poko, J. Mass Transport and Thermal Conductivity Properties of Flax Shives for Use in Construction Industry. *J. Nat. Fibers* **2021**, *18*, 995–1006. [CrossRef]
11. Kosiński, P.; Brzyski, P.; Suchorab, Z.; Łagód, G. Heat Losses Caused by the Temporary Influence of Wind in Timber Frame Walls Insulated with Fibrous Materials. *Materials* **2020**, *13*, 5514. [CrossRef]
12. Balčiūnas, G.; Vėjelis, S.; Lekūnaitė, L.; Kremensas, A. Assessment of structure influence on thermal conductivity of hemp shives composite. *Environ. Eng. Manag. J.* **2016**, *15*, 699–705. [CrossRef]
13. Bourdot, A.; Moussa, T.; Gacoin, A.; Maalouf, C.; Vazquez, P.; Thomachot-Schneider, C.; Bliard, C.; Merabtine, A.; Lachi, M.; Douzane, O.; et al. Laboratory Characterization of a hemp-based agro-material: Influence of starch ratio and hemp shive size on physical, mechanical, and hygrothermal properties. *Energy Build.* **2017**, *153*, 501–512. [CrossRef]
14. Rahim, M.; Douzane, O.; Tran Le, A.D.; Promis, G.; Laidoudi, B.; Crigny, A.; Dupre, B.; Langlet, T. Characterization of flax lime and hemp lime concretes: Hygric properties and moisture buffer capacity. *Energy Build.* **2015**, *88*, 91–99. [CrossRef]
15. Collet, F.; Chamoin, J.; Pretot, S.; Lanos, C. Comparison of the hygric behaviour of three hemp concretes. *Energy Build.* **2013**, *62*, 294–303. [CrossRef]
16. Jiang, Y.; Ansell, M.; Jia, X.; Hussain, A.; Lawrence, M. Physical characterisation of hemp shiv: Cell wall structure and porosity. In Proceedings of the 2nd International Conference on Bio-Based Building Materials, Clermont-Ferrand, France, 21–23 June 2017.
17. Nguyen, T.; Picandet, V.; Amziane, S.; Baley, C. Influence of compactness and hemp hurd characteristics on the mechanical properties of lime and hemp concrete. *Eur. J. Environ. Civ. Eng.* **2009**, *13*, 1039–1050. [CrossRef]
18. Sinka, S.; Sahmenko, G.; Korjakins, A.; Bajare, D. Lime-hemp concrete (LHC) enhancement using magnesium based binders. *Acad. J. Civ. Eng.* **2017**, *35*, 238–245. [CrossRef]
19. Sinka, S.; Sahmenko, G.; Korjakins, A.; Radina, L.; Bajare, D. Hemp Thermal Insulation Concrete with Alternative Binders, Analysis of their Thermal and Mechanical Properties. *IOP Conf. Ser. Mater. Sci. Eng.* **2015**, *96*, 012029. [CrossRef]
20. Dinh, T.M.; Magniont, C.; Coutand, M.; Escadeillas, G. Hemp concrete using innovative pozzolanic binder. *Acad. J. Civ. Eng.* **2015**, *33*, 265–270.
21. Cerezo, V. Propriétés mécaniques, Thermiques et Acoustiques d'un Matériau à Base de Particules Végétales: Approche Expérimentale et Modélisation théorique. Ph.D. Thesis, National School of State Public Works, Vaulx-en-Velin, France, 2005.
22. Magniont, C. Contribution à la Formulation et à la Caractérisation d'un Écomatériau de Construction à Base D'agroressources. Ph.D. Thesis, Université de Toulouse, Toulouse, France, 2010.
23. Verdier, T. Valorisation de granulats végétaux dans un matériau de construction à matrice minérale. Master's Thesis, Université de Toulouse, Toulouse, France, 2012.
24. Brzyski, P.; Gleń, P.; Gładcki, M.; Rumińska, M.; Suchorab, Z.; Łagód, G. Influence of the Direction of Mixture Compaction on the Selected Properties of a Hemp-Lime Composite. *Materials* **2021**, *14*, 4629. [CrossRef]
25. Arnaud, L.; Gourlay, E. Experimental study of parameters influencing mechanical properties of hemp concretes. *Constr. Build. Mater.* **2012**, *28*, 50–56. [CrossRef]
26. Benfratello, S.; Capitano, C.; Peri, G.; Rizzo, G.; Scaccianoce, G.; Sorrentino, G. Thermal and structural properties of a hemp-lime biocomposite. *Constr. Build. Mater.* **2013**, *48*, 745–754. [CrossRef]

27. Walker, R.; Pavia, S. Moisture transfer and thermal properties of hemp–lime concretes. *Constr. Build. Mater.* **2014**, *64*, 270–276. [[CrossRef](#)]
28. Stevulova, N.; Kidalova, L.; Cigasova, J.; Junak, J.; Sicakova, A.; Terpakova, E. Lightweight Composites Containing Hemp Hurds. *Proced. Eng.* **2013**, *65*, 69–74. [[CrossRef](#)]
29. Walker, R.; Pavia, S.; Mitchell, R. Mechanical properties and durability of hemp–lime concretes. *Constr. Build. Mater.* **2014**, *61*, 340–348. [[CrossRef](#)]
30. Barclay, M.; Holcroft, N.; Shea, A.D. Methods to determine whole building hygrothermal performance of hempelime buildings. *Build. Environ.* **2014**, *80*, 204–212. [[CrossRef](#)]
31. Tran Le, A.; Maalouf, C.; Mai, T.H.; Wurtz, E.; Collet, F. Transient hygrothermal behaviour of a hemp concrete building envelope. *Energy Build.* **2010**, *42*, 1797–1806. [[CrossRef](#)]
32. Brzyski, P.; Gładcki, M.; Rumińska, M.; Pietrak, K.; Kubiś, M.; Łapka, P. Influence of Hemp Shives Size on Hygro-Thermal and Mechanical Properties of a Hemp-Lime Composite. *Materials* **2020**, *13*, 5383. [[CrossRef](#)]
33. Iştoan, R.F.; Manea, D.L.; Tamas-Gavrea, D.R.; Rosca, I.C. Hemp-clay building materials—An investigation on acoustic, thermal and mechanical properties. *Procedia Manuf.* **2019**, *32*, 216–223. [[CrossRef](#)]
34. Hamzaoui, R.; Guessasma, S.; Abahri, K. Mechanical performance of mortars modified with hemp fibres, shives and milled fly ashes. In Proceedings of the 2nd International RILEM/COST Conference on Early Age Cracking and Serviceability in Cement-Based Materials and Structures—EAC2, ULB-VUB, Brussels, Belgium, 12–14 September 2017.
35. Mostefai, N.; Hamzaoui, R.; Guessasma, S.; Aw, A.; Nouri, H. Microstructure and mechanical performance of modified hemp fibre and shiv mortars: Discovering the optimal formulation. *Mater. Des.* **2015**, *84*, 359–371. [[CrossRef](#)]
36. Hamzaoui, R.; Guessasma, S.; Abahri, K.; Bouchenafa, O. Formulation of Modified Cement Mortars Using Optimal Combination of Fly Ashes, Shiv, and Hemp Fibers. *J. Mater. Civ. Eng.* **2020**, *32*, 04019354. [[CrossRef](#)]
37. Jiang, Y.; Lawrence, M.; Ansell, M.P.; Hussain, A. Cell wall microstructure, pore size distribution and absolute density of hemp shiv. *R. Soc. Open Sci.* **2018**, *5*, 4. [[CrossRef](#)]
38. Shen, X.; Jiang, P.; Guo, D.; Li, G.; Chu, F.; Yang, S. Effect of Furfurylation on Hierarchical Porous Structure of Poplar Wood. *Polymers* **2021**, *13*, 32. [[CrossRef](#)]
39. Zhao, J.; Yang, L.; Cai, Y. Combining mercury intrusion porosimetry and fractal theory to determine the porous characteristics of wood. *Wood Sci. Technol.* **2021**, *55*, 109–124. [[CrossRef](#)]
40. Wójcik, R.; Tunkiewicz, M. Ink-bottle pores—characteristics, methods of determination on the basis of lime–cements mortar. *Mater. Bud.* **2017**, *10*, 59–61. (In Polish) [[CrossRef](#)]
41. EN 12667: Thermal Performance of Building Materials and Products—Determination of Thermal Resistance by Means of Guarded Hot Plate and Heat Flow Meter Methods—Products of High and Medium Thermal Resistance. Available online: <https://standards.iteh.ai/catalog/standards/sist/c479b508-30f0-4315-aa53-ce8f39252a5f/sist-en-12667-2002> (accessed on 11 February 2022).
42. Kosiński, P.; Wójcik, R. An Impact of Air Permeability on Heat Transfer through Partitions Insulated with Loose Fiber Materials. *Appl. Mech. Mater.* **2017**, *861*, 190–197. [[CrossRef](#)]
43. Zach, J.; Slávik, R.; Novák, V. Investigation of the Process of Heat Transfer in the Structure of Thermal Insulation Materials Based on Natural Fibres. *Procedia Eng.* **2016**, *151*, 352–359. [[CrossRef](#)]
44. Delhomme, F.; Hajimohammadi, A.; Almeida, A.; Jiang, C.; Moreau, D.; Gan, Y.; Wang, X.; Castel, A. Physical properties of Australian hurd used as aggregate for hemp concrete. *Mater. Today Commun.* **2020**, *24*, 100986. [[CrossRef](#)]
45. Brzyski, P.; Kosiński, P.; Skoratko, A.; Motacki, W. Thermal properties of cellulose fiber as insulation material in a loose state. *AIP Conf. Proc.* **2019**, *2133*, 020006. [[CrossRef](#)]
46. Kosiński, P.; Brzyski, P.; Szewczyk, A.; Motacki, W. Thermal properties of raw hemp fiber as a loose-fill insulation material. *J. Nat. Fib.* **2018**, *15*, 717–730. [[CrossRef](#)]
47. Kosiński, P.; Wójcik, R.; Skoratko, D.; Attia, S. An impact of moisture content on the air permeability of the fibrous insulation materials. *J. Phys. Conf. Ser.* **2021**, *2069*, 012205. [[CrossRef](#)]
48. Csanády, D.; Fenyvesi, O.; Nagy, B. Heat Transfer in Straw-Based Thermal Insulating Materials. *Materials* **2021**, *14*, 4408. [[CrossRef](#)]
49. ISO 10456; Building Materials and Products—Hygrothermal Properties—Tabulated Design Values and Procedures for Determining Declared and Design Thermal Values. British Standards: London, UK, 2008.
50. Kosiński, P.; Wójcik, R.; Semen, B. Experimental study on the deterioration of thermal insulation performance due to wind washing of the cavity insulation in leaky walls. *Sci. Technol. Built Environ.* **2019**, *25*, 1164–1177. [[CrossRef](#)]